Short Communication

Quantification of threonine-containing lysophospholipids using ESI-LC-MS/MS in mouse tissues

Michiyo Okudaira[1,2], Kuniyuki Kano[2], Kumiko Makide[3], Daisuke Saigusa[4], Tomohiko Ohwada[2], Junken Aoki[2*]

[1]Faculty of Hospital Pharmacy, Teikyo University, 2−11−1 Kaga, Itabashi-ku, Tokyo 173−8605, Japan
[2]Department of Health Chemistry, Graduate School of Pharmaceutical Sciences, The University of Tokyo, 7−3−1 Hongo, Bunkyo-ku, Tokyo 113−0033, Japan
[3]Laboratory of Molecular and Cellular Biochemistry, Graduate School of Pharmaceutical Sciences, Tohoku University, 6−3 Aoba, Aramaki, Aoba-ku, Sendai 980−8578, Japan
[4]Laboratory of Biomedical and Analytical Sciences, Faculty of Pharma-Sciences, Teikyo University, 2−11−1 Kaga, Itabashi-ku, Tokyo 173−8605, Japan

Abstract Lysophosphatidylthreonine (LysoPT) is a potent inducer of mast cell degranulation that was previously identified as an analog of a bioactive lysophospholipid, lysophoshatidylserine (LysoPS). However, it remains to be solved if LysoPT is present *in vivo*. In the present study, we tried to detect LysoPT in biological samples using liquid chromatography/tandem mass spectrometry (LC-MS/MS) and examined its tissue distribution. In several mouse tissues, we detected LysoPT as a mixture of LysoPT with several different fatty acid chains, *i.e.*, LysoPT species. C18:0-LysoPT was a major LysoPT species in various tissues and plasma with the highest expression in the stomach. The fatty acid species and tissue distributions of LysoPS and LysoPT were similar, suggesting that the two lysophospholipids share a common synthetic pathway. The present study indicates that LysoPT behaves as an endogenous lysophospholipid mediator.

Key words: lysophosphatidylthreonine, LysoPT, lysophosphatidylserine, LysoPS, LC-MS/MS, lysophospholipid mediator

Introduction

Mast cells are involved in developing immediate allergic reactions by releasing various inflammatory mediators such as histamine and serotonin stored in their cytoplasmic granules in response to an antigen. Administration of lysophosphatidylserine (LysoPS), a kind of lysophospholipids, has been shown to potentiate the antigen-induced histamine release (degranulation) from rodent mast cells both *in vivo* and *in vitro*[1−4]. However, we poorly understand the role of LysoPS in activating mast cells in pathophysiological contexts. We previously synthesized a series of LysoPS analogs with modifications in either the glycerol backbone, acyl chain, or ester bond of LysoPS. We showed that one of them, lysophosphatidylthreonine (LysoPT), which has a methyl group at the β-carbon of serine, was much more potent in inducing mast cell degranulation than LysoPS [5,6]. LysoPT induced histamine release from mast cells *in vitro* and *in vivo* at a concentration less than one-tenth of LysoPS. Like LysoPS, LysoPT also induced hypothermia and anaphylactic shock in mice. Injection of LysoPT into mice caused transient decreases of body temperature at a concentration 50-fold lower than that of LysoPS, raising the possibility that LysoPT functions as a lipid mediator[5].

Despite its potent pharmacological activities to induce mast cell degranulation, hypothermia, and anaphylactic shock, little is known about the presence of LysoPT *in vivo*.

*Corresponding author
Junken Aoki
Department of Health Chemistry, Graduate School of Pharmaceutical Sciences, The University of Tokyo, 7−3−1 Hongo, Bunkyo-ku, Tokyo 113−0033, Japan
Tel: +81−3−5841−4720, Fax: +81−3−5841−0280
E-mail: jaoki@mol.f.u-tokyo.ac.jp
Received: August 12, 2022. Accepted: October 27, 2022.
Epub November 16, 2022.
DOI: 10.24508/mms.2022.11.008

In addition, the synthetic pathway of LysoPT has been unknown. Other glycero-lysophospholipids, such as lysophosphatidic acid (LPA) and LysoPS, are known to be produced from their precursors, including phosphatidic acid (PA), phosphatidylserine (PS), and lysophosphatidylcholine (LPC) by several kinds of phospholipases[7–9]. Interestingly, phosphatidylthreonine (PT), which is a plausible precursor of LysoPT, has been shown to be present in tissues from various species, including rat brain[10], hippocampal neurons[11], and the endoplasmic reticulum of Toxoplasma gondii[12]. Various phospholipase A_1 and A_2 types are present, indicating that LysoPT is present *in vivo*.

Our previous study developed a liquid chromatography/tandem mass spectrometry (LC-MS/MS) method to analyze lysophospholipids[13]. However, due to the lower sensitivity, we could not detect LysoPT in biological samples. In the present study, we changed the mass spectrometry (MS) instrument and optimized the method for LysoPT analysis. The new method makes it possible to detect and quantify LysoPT concentrations as low as 500 pM. In addition, the method is helpful for examining the tissue distribution of LysoPS in mice. The present method may help to understand the pathophysiological roles of LysoPT and LysoPS as lipid mediators.

Materials and Methods

Chemicals

LysoPS standards (C16:0-LysoPS, C18:0-LysoPS, C18:1-LysoPS) and internal standard, C17:1-LysoPS, were purchased from Avanti Polar Lipids. C16:0-LysoPT, C18:0-LysoPT, and C18:1-LysoPT were chemically synthesized previously[5] and used as LysoPT standards. Methanol (CH_3OH) and acetonitrile (CH_3CN) of LC/MS grade were obtained from Kanto Chemical (Tokyo, Japan). Ammonium formate ($HCOONH_4$) of LC/MS grade was obtained from Wako Pure Chemical Industries. Ultra grade water was prepared with Milli-Q Advantage A 10 Ultrapure Water Purification System from Millipore.

Animals

Male C57 BL/6 mice (8−12 weeks) were used. Mice were purchased from Japan SLC and maintained according to the Guidelines of Animal Experimentation of The University of Tokyo. The animal protocol was approved by the Institutional Animal Care and Use Committee at the University of Tokyo.

Sample preparation

For plasma preparation, blood was collected using a heparinized capillary and centrifuged at 1,500×*g* for 10 min at 4°C. The resulting supernatant was used as plasma. For serum preparation, blood was collected using a non-coated capillary and was incubated for 1 h at 37°C to induce blood coagulation. Then it was kept at 4°C for 4 h to retract the blood clots and was centrifuged at 1,500×*g* for 10 min at 4°C. The resulting supernatant was used as a serum.

A 10 μL of plasma and serum samples were mixed with 100 μL of CH_3OH containing 100 nM C17:1-LysoPS in a 1.5 mL siliconized sample tube. It was sonicated in a water bath-type sonicator to recover lipids in CH_3OH. The extracts were sequentially centrifuged at 21,500×*g*, and the resulting supernatant was passed through an acetyl cellulose filter (pore size 0.22 μm). A volume of 10 μL of samples was injected into LC-MS/MS.

For tissue samples, mice were rapidly perfused transcardially with cold PBS through the left ventricle, and subsequently, tissues were collected. 5−10 mg tissues were transferred to 2.0 mL sample tubes, and 10-fold volume CH_3OH containing 100 nM C17:1-LysoPS and beads were added for homogenization using an MS-100R beads cell disrupter. The extracts were sequentially centrifuged at 1,500×*g* and 21,500×*g*, and the resulting supernatant was passed through a filter. A volume of 10 μL of the sample was injected into LC-MS/MS.

Liquid chromatography system and conditions

This study used the A NANO SPACE SI-2 LC system (Osaka-soda, Tokyo, Japan). The system consists of dual pumps, an autosampler, a column oven, and an online degasser. The chromatographic separation was performed on CAPCELL PAK C18 ACR (250 mm×1.5 mm i.d., 3 μm particle size) (Osaka-soda, Tokyo, Japan) analytical column coupled with a CAPCELL PAK C18 ACR (10 mm×2.0 mm i.d., 3 μm particle size) guard column maintained at 40°C. The flow rate was 150 μL min^{-1}, and the mobile phases were formed using 5 mM $HCOONH_4$ (H_2O/CH_3CN=100/0, v/v) as eluent A and 5 mM $HCOONH_4$ (H_2O/CH_3CN=5/95, v/v) as eluent B whereby the solutions were adjusted to pH 4.0 using HCOOH, respectively. The liquid chromatography (LC) analysis started with 50% B for 0.2 min, followed by a linear gradient from 50 to 100% B in 12.0 min and maintenance of 100% B for 5 min. Subsequently, the mobile phase was immediately returned to the initial condi-

tions and maintained for 3 min until the end of the run. A divert valve was used to divert the LC effluent to the waste during the first 5 min and the last 2 min.

Mass spectrometry system and conditions

The MS system was a Thermo Fischer Scientific TSQ Quantiva triple quadrupole mass spectrometer with a heated electrospray ionization (HESI) source. The operating condition was optimized for C18:1-LysoPS, dissolved with CH_3OH (1 μM) by continuously infusing at a 5 μL min^{-1}. The HESI spray voltage was 2,500 V, the heated ion transfer tube temperature was 329°C, the sheath gas pressure was 38 psi, the auxiliary gas pressure was 12 psi, and the heated vaporizer temperature was 279°C. Both the sheath gas and the auxiliary gas were nitrogen gas. The collision gas was argon at a pressure of 2.0 mTorr. HESI was performed in a negative ion mode. The optimized HESI of seven LysoPS species (C16:0, C18:0, C18:1, C18:2, C20:4, C22:6, and C17:1 (used as internal standard)) and of three LysoPT species (C16:0, C18:0, and C18:1) produced abundant $[M-H]^-$ ions at *m/z* 496.3, 524.3, 522.3, 520.3, 544.3, 568.3, 508.3, 510.3, 538.3 and 536.3, respectively. Samples were analyzed by the selected reaction monitoring (SRM) mode, employing the transition of the $[M-H]^-$ precursor ions to their product ions. For the MS/MS analysis, the collision energies for collision-induced dissociation of LysoPS and LysoPT were 19 eV. In SRM mode, the transitions of the precursor ion into the production were monitored: *m/z* 496.3 → 409.3 for C16:0-LysoPS, *m/z* 524.3 → 437.3 for C18:0-LysoPS, *m/z* 522.3 → 435.3 for C18:1-LysoPS, *m/z* 520.3 → 433.3 for C18:2-LysoPS, *m/z* 544.3 → 457.3 for C20:4-LysoPS, *m/z* 568.3 → 481.3 for C22:6-LysoPS, *m/z* 508.3 → 421.2 for C17:1-LysoPS, *m/z* 510.3 → 409.3 for C16:0-LysoPT, *m/z* 538.3 → 437.3 for C18:0-LysoPT and *m/z* 536.3 → 435.3 for C18:1-LysoPT. The LC-MS/MS system was controlled by the Xcalibur software (Thermo Fisher Scientific) and data were collected with the same software.

Method validation

A mixture of LysoPS species (C16:0, C18:0, and C18:1, each 1 μM) and LysoPT species (C16:0, C18:0, and C18:1, each 1 μM) was prepared as a CH_3OH solution. It was diluted with CH_3OH to prepare six standard solutions with final concentrations of 100 nM, 50 nM, 10 nM, 5 nM, 1 nM, and 500 pM, respectively, each containing 100 nM C17:1-LysoPS as internal standard. 10 μL of each standard solution was injected into LC-MS/MS. The ratio between analytes and the internal standard peak area was calculated for quantification.

We determined the precision of the present method by analyzing six samples containing the same concentration of LysoPS and LysoPT on the same day (intra-day analysis). This procedure was repeated for three days (inter-day analysis). The coefficient of variation within one sample run (intra-day) and between sample runs (inter-day) was determined for various concentrations of LysoPS and LysoPT. To determine the recovery, a mixture of LysoPT species (C16:0, C18:0, and C18:1) at 50 nM and 100 nM were prepared and added to the mouse tissue homogenates (brain, thymus, heart, lung, liver, spleen, kidney, stomach, small intestine, muscle and skin, ten mg each) or plasma (10 μL). Lipids were extracted by adding 90 μL CH_3OH containing internal standard (C17:1-LysoPS). The samples for MS injection were prepared as described above. The extraction recovery was calculated by the following formula: [(detected concentration-endogenous concentration)/standard concentration]×100 (%).

Results

LC-MS/MS analysis of LysoPT

Previously, we constructed a system to quantify various lysophospholipids, including LysoPS, in biological samples using LC-MS/MS[13]. However, using this method, we could not detect LysoPT, possibly because it was not sufficiently sensitive. In the previous study, we used TSQ Quantum Ultra mass spectrometer (Thermo Fischer Scientific) mass system. Subsequently, we used a high-performance TSQ Quantiva mass spectrometer (Thermo Fischer Scientific) for the detection of LysoPT. For the Quantiva analyses, we first performed product ion scanning using a chemically synthesized C18:1-LysoPT[5]. The product ion scanning analyses indicated that deprotonated precursor ions of C18:1-LysoPT (*m/z* 536.3) lost the corresponding polar head group (*i.e.* threonine) upon collisional activation, yielding a characteristic fragment ion of C18:1-LPA (*m/z* 435.3). The fragmentation was useful for SRM detection of LysoPT in the LC-MS/MS analyses. We could also detect and analyze LysoPS species using Quantiva by the same strategy.

Typical SRM chromatograms of LysoPT and LysoPS standards were obtained by LC-MS/MS analyses (Fig. 1A and 1C). This method was applied to mouse large-intestine

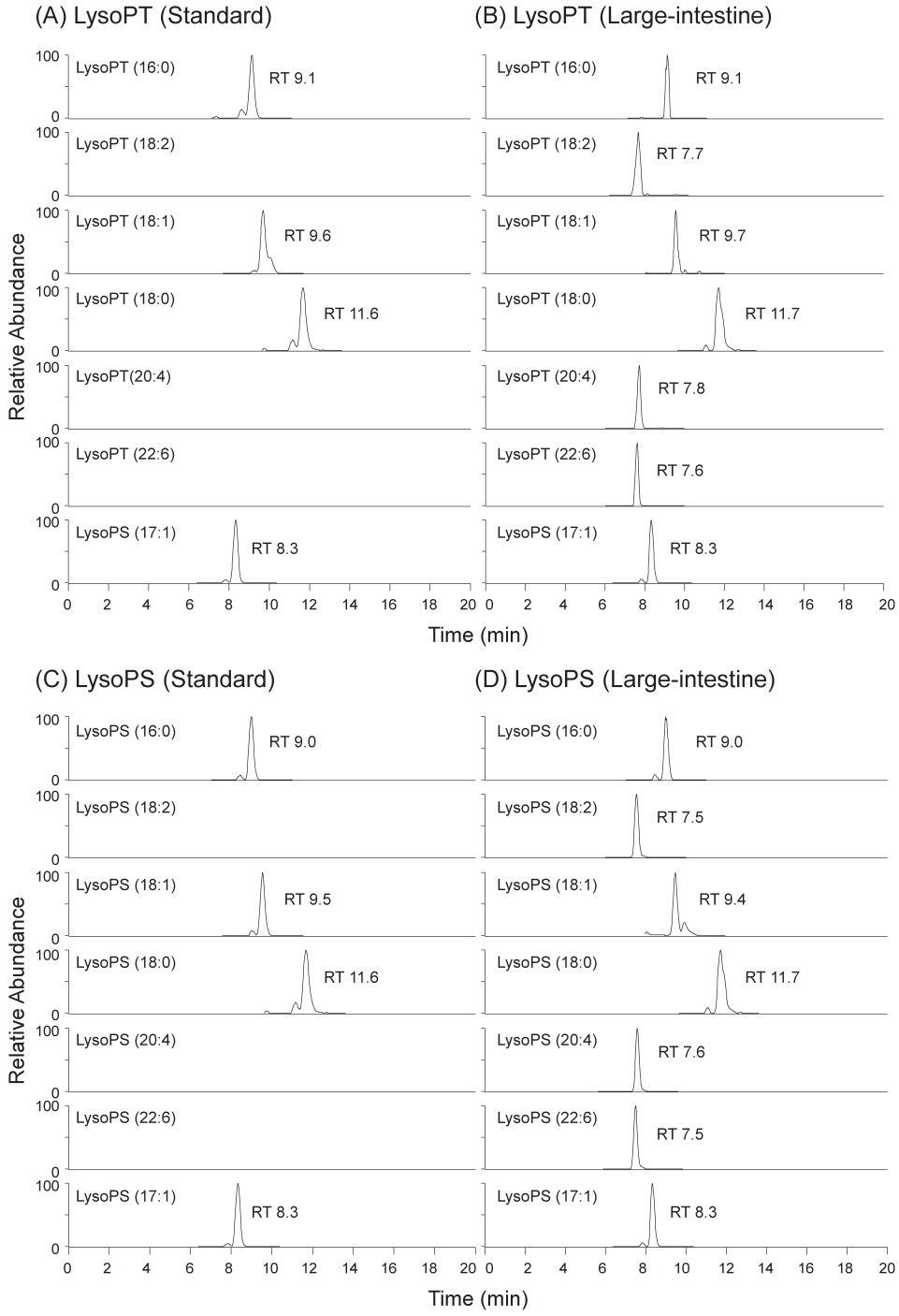

Fig. 1. (A, C) SRM chromatograms of LysoPT (A) standard samples (C16:0, C18:1 and C18:0, each 50 pmol), LysoPS (C) standard samples (C16:0, C18:1 and C18:0, each 50 pmol). (B, D) LysoPT species (C16:0, C18:2, C18:1, C18:0, C20:4 and C22:6) (B) and LysoPS species (C16:0, C18:2, C18:1, C18:0, C20:4 and C22:6) (D) detected in the mouse large intestine.

For the large-intestine sample, lipid extract corresponding to 10 mg of large-intestine tissue was injected. The retention times for each LysoPT and LysoPS species were similar between the standard samples and large-intestine sample.

homogenates (Fig. 1B and 1D). Peaks with *m/z* values and retention time that correspond to C16:0-LysoPT, C18:0-LysoPT, and C18:1-LysoPT standards were detected in the mouse large-intestine homogenates. Thus, we concluded that LysoPT species with C16:0, C18:0, and C18:1 were present in mice.

Method validation

Linearity

The linearity of the calibration curves was evaluated by determining the ion intensity of analytes in eight concentrations (50 pM, 100 pM, 500 pM, 1 nM, 5 nM, 10 nM, 50

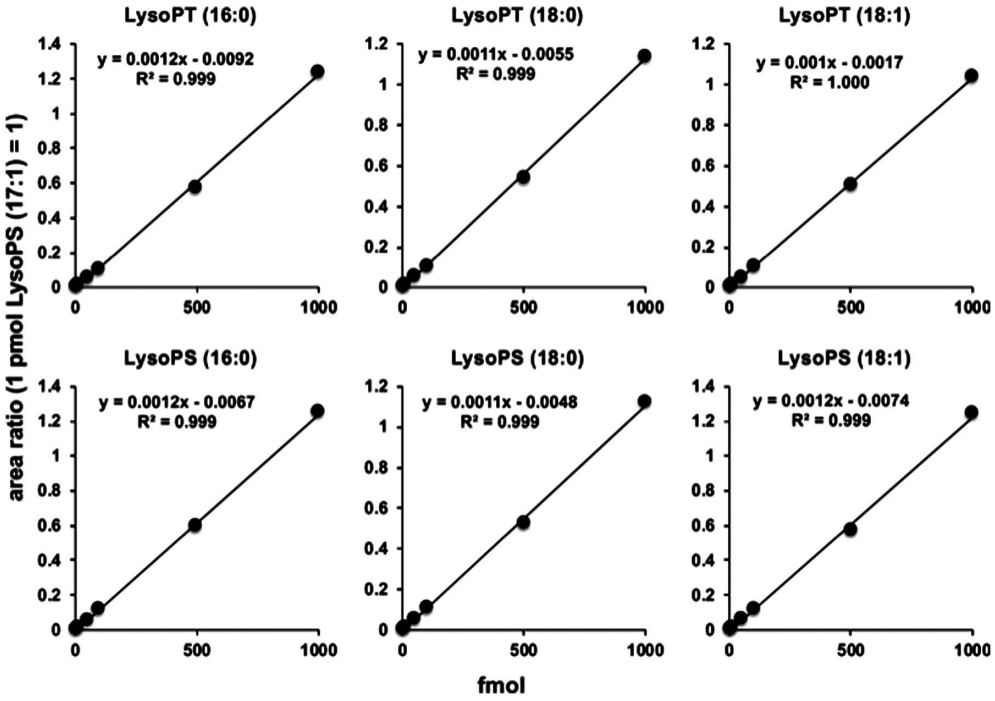

Fig. 2. Standard curves of LysoPT and LysoPS.
The curves were constructed by plotting the peak area ratio of the analytes at six concentrations (500 pM, 1 nM, 5 nM, 10 nM, 50 nM and 100 nM, *n*=6, each) against the concentrations of the internal standard (C17:1-LysoPS). The precisions of the method are shown in Table 1.

nM, and 100 nM). The calibration curves of C16:0-LysoPT, C18:0-LysoPT, and C18:1-LysoPT were linear from 500 pM (5 fmol) to 100 nM (1000 fmol) (Fig. 2). Similarly, C16:0-LysoPS, C18:0-LysoPS, and C18:1-LysoPS were detected with linearity from 500 pM (5 fmol) to 100 nM (1000 fmol) (Fig. 2). The present method enables us to detect both LysoPT and LysoPS at 20-fold lower concentrations compared with the previous method. When we tested 50 pM (0.5 fmol), we could not detect C16:0-LysoPT, C18:0-LysoPT, and C18:1-LysoPT (data not shown). At 100 pM (1 fmol), we could detect C16:0-LysoPT and C18:0-LysoPT with signal to noise ratio over 30 but could not detect C18:1-LysoPT (data not shown). The linearity was observed from 500 pM and 100 nM for the three LysoPT species (Fig. 2). Thus, the lower limit of quantification (LLOQ) and the lower limit of detection (LLOD) for C16:0-LysoPT or C18:0-LysoPT is 100 pM and those for C18:1-LysoPT is 500 pM.

Assay precision

The intra- and inter-day precision of the assay was investigated by determining the level of LysoPT and LysoPS in the standard solutions containing 500 pM, 1 nM, 5 nM, 10 nM, 50 nM, and 100 nM LysoPT and LysoPS in addition to the internal standard (100 nM C17:1-LysoPS). Most intra- and inter-day precision values were less than 10% (Table 1), confirming the accuracy and robustness of the present assay method (Table 1).

Recovery

We examined the recovery of the assay by spiking samples with a known amount of LysoPT and determined the amount of recovered LysoPT by LC-MS/MS. The recoveries were in the ranges 91.0−119.7% for C16:0-LysoPT, 81.2−122.8% for C18:0-LysoPT, and 91.7−121.0% for C18:1-LysoPT (Table 2).

LysoPT and LysoPS distribution in mouse tissues

We then determined the distribution of LysoPT and LysoPS in mice using the established method. Several LysoPT species (C16:0, C18:0, C18:1, C18:2, C20:4, and C22:6) and LysoPS species (C16:0, C18:0, C18:1, C18:2, C20:3, C20:4, C20:5, and C22:6) species were detected in the samples (brain, thymus, heart, lung, liver, spleen, kidney, stomach, small intestine, large intestine, muscle, skin, plasma, and serum) (Fig. 3A and Table 3). Both saturated and unsaturated LysoPT and LysoPS species were detected, indicating that both phospholipase A_1s and phospholipase A_2s are

Table 1. Precision of assays of each LysoPT and LysoPS species

Intra-day precision (%)

concentration (nM)	fmol		LysoPT (16:0)	LysoPT (18:0)	LysoPT (18:1)	LysoPS (16:0)	LysoPS (18:0)	LysoPS (18:1)
0.5	5		7.1	1.8	10.3	9.9	7.1	4.0
1	10		6.4	5.3	1.9	7.8	5.9	9.9
5	50		2.1	6.1	0.8	9.4	2.5	6.2
10	100		5.7	6.9	3.1	5.0	5.6	9.3
50	500		3.2	5.3	0.7	2.9	6.5	1.3
100	1000		4.1	3.8	2.4	0.7	2.6	0.6

Inter-day precision (%)

concentration (nM)	fmol		LysoPT (16:0)	LysoPT (18:0)	LysoPT (18:1)	LysoPS (16:0)	LysoPS (18:0)	LysoPS (18:1)
0.5	5		9.2	1.9	1.7	4.5	3.7	6.0
1	10		4.0	2.8	4.0	3.2	1.6	8.0
5	50		0.8	1.4	4.2	2.2	1.3	5.1
10	100		1.7	2.1	4.4	3.5	1.7	3.1
50	500		3.0	1.5	1.5	0.9	3.3	3.6
100	1000		5.0	0.9	1.9	2.3	2.5	2.1

Data are SD among intra-day or inter-day (n=6).

Table 2. Extraction recovery of three LysoPT species from several tissues

		Brain	Thymus	Heart	Lung	Liver	Spleen	Kidney	Stomach	Intestine	Mascle	Skin	Plasma
LysoPT	50 nM	107.7	106.8	104.1	107.1	112.5	102.4	116.1	119.7	98.7	109.1	97.6	91.0
(16:0)	100 nM	101.0	98.9	107.7	109.8	110.9	104.8	113.6	106.4	98.4	111.5	105.0	103.2
LysoPT	50 nM	116.7	81.2	102.1	93.1	103.0	95.4	118.4	111.9	82.6	110.3	113.7	107.5
(18:0)	100 nM	113.6	86.1	95.5	84.2	102.8	92.9	109.4	115.2	107.1	109.0	122.8	94.0
LysoPT	50 nM	111.0	103.0	105.0	108.1	114.3	97.9	111.4	121.0	101.0	113.1	109.6	92.8
(18:1)	100 nM	106.6	101.0	103.9	107.5	91.7	104.1	112.9	111.4	114.2	120.2	112.0	108.9

Data are mean (n=3).

involved in the production of LysoPT and LysoPS. LysoPT and LysoPS levels were high in digestive tissues (stomach, large and small intestines) and kidneys. Patterns of LysoPT species expression differed between tissues (Fig. 3B). LysoPT appeared to be most highly expressed in the stomach, followed by the large intestine. In these tissues, C18:0-LysoPT was the main LysoPT species (Fig. 3A and B).

Like LysoPT, LysoPS was detected in all tissues tested (Fig. 3B and C). Interestingly, the composition of LysoPS and LysoPT species was similar in each organ. For example, C18:0-LysoPS and C18:0-LysoPT were the most abundant species in the stomach and kidney, followed by the C16:0- and C18:1-species of LysoPS and LysoPT. In the large intestine, C18:0-LysoPT and C18:0-LysoPS were the most common molecular species. In contrast, the relative concentrations of LysoPT and LysoPS varied among the tissues. For example, in the lung, spleen, kidney, small intestine, large intestine, and skin, the ratio of LysoPS to LysoPT was roughly 100:1, while in the heart, muscle, brain, and liver/stomach, it was roughly 30:1, 60:1, 250:1 and 400:1, respectively.

LysoPT species, especially with unsaturated fatty acids (arachidonic (C20:4) and docosahexaenoic (C22:6) acids), were detected in the serum, while they were not detected in the plasma (Fig. 3D), suggesting that they were produced during the blood coagulation. LysoPS was detected in both plasma and serum, with concentrations in serum approximately 50-fold higher than in plasma. The fact that LysoPT was not detected in plasma is likely because LysoPT was below the detection limit. Interestingly, the LysoPS species in serum and plasma differed significantly (Fig. 3D). In plasma, C18:0-LysoPS were the main LysoPS species,

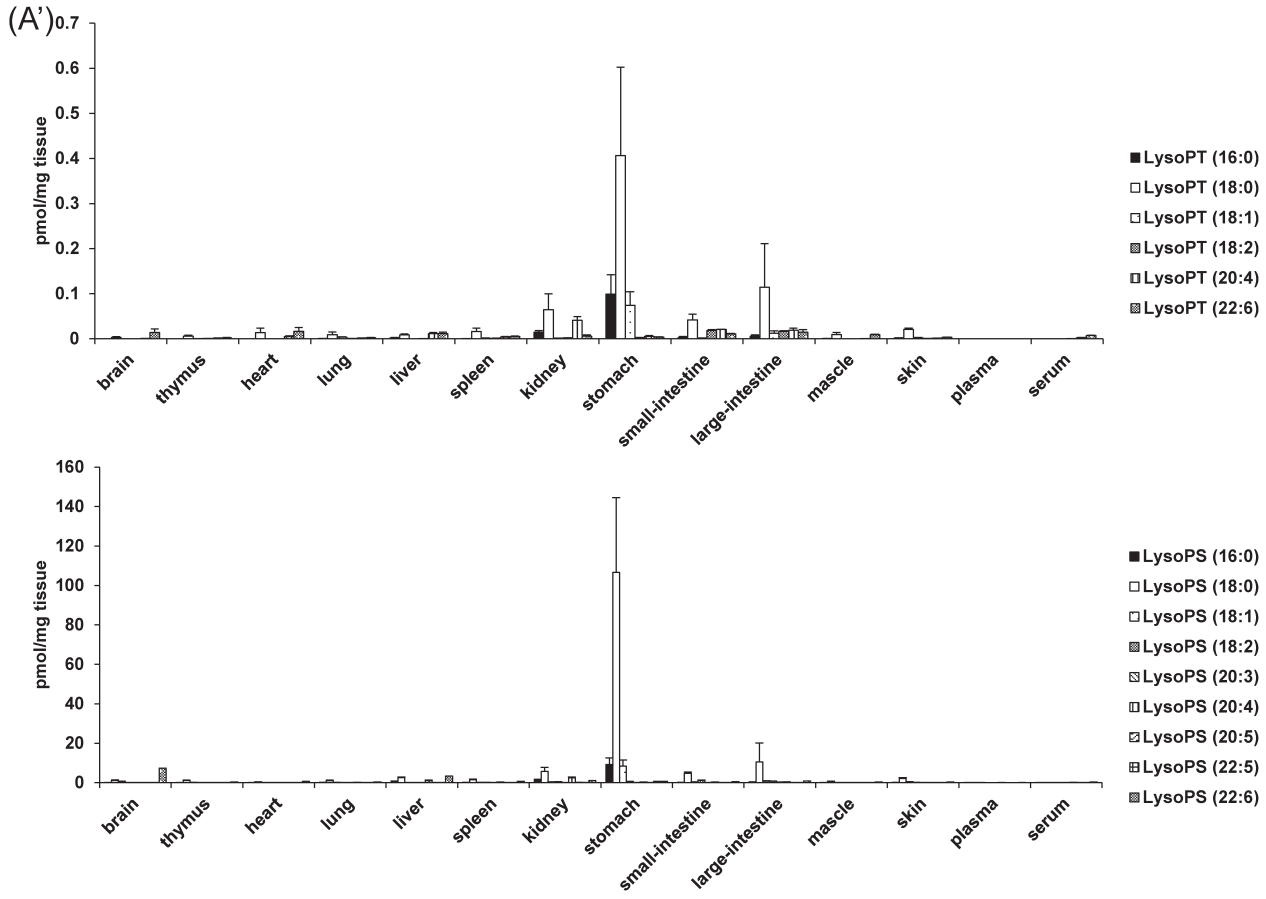
(A')
pmol/mg tissue
brain
thymus
heart
lung
liver
spleen
kidney
stomach
small-intestine
large-intestine
mascle
skin
plasma
serum
LysoPT (16:0)
LysoPT (18:0)
LysoPT (18:1)
LysoPT (18:2)
LysoPT (20:4)
LysoPT (22:6)
LysoPS (16:0)
LysoPS (18:0)
LysoPS (18:1)
LysoPS (18:2)
LysoPS (20:3)
LysoPS (20:4)
LysoPS (20:5)
LysoPS (22:5)
LysoPS (22:6)

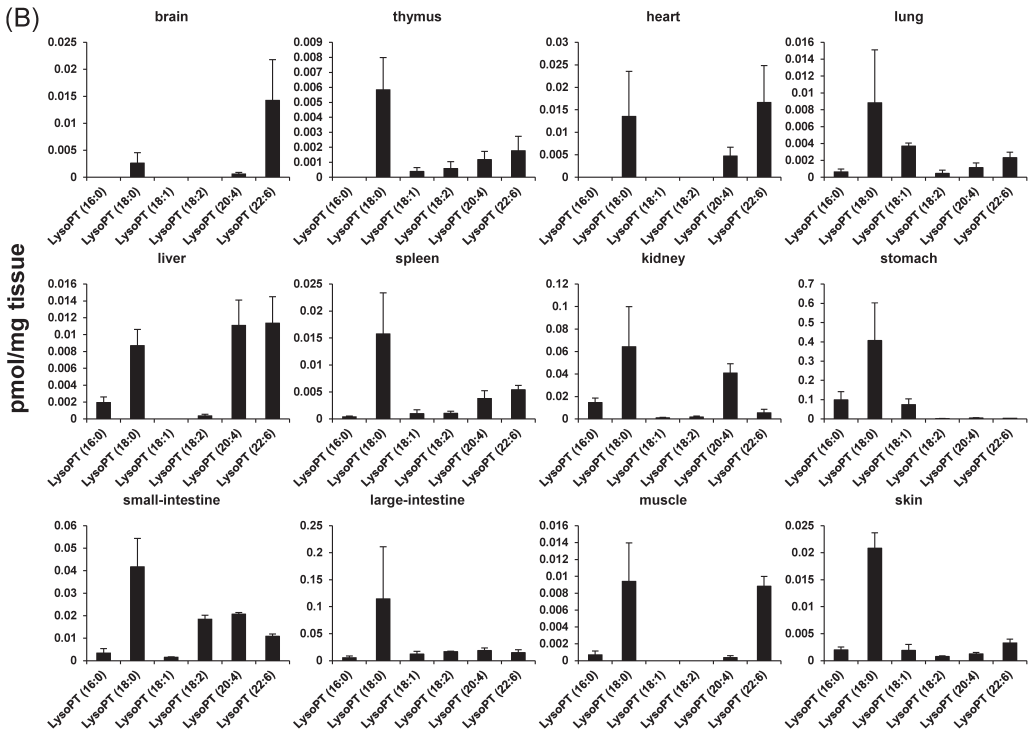
(B)
pmol/mg tissue
brain
thymus
heart
lung
liver
spleen
kidney
stomach
small-intestine
large-intestine
muscle
skin
LysoPT (16:0)
LysoPT (18:0)
LysoPT (18:1)
LysoPT (18:2)
LysoPT (20:4)
LysoPT (22:6)

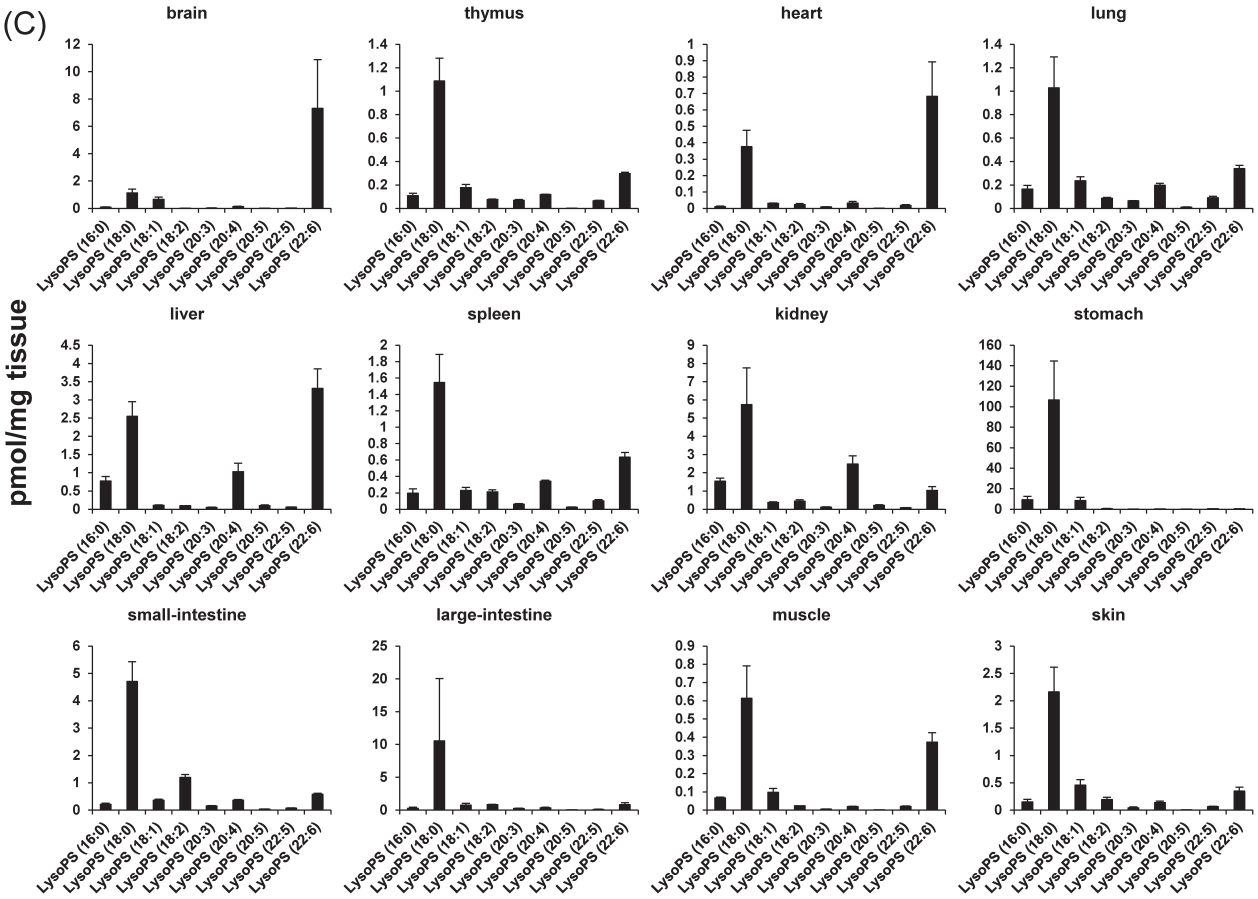

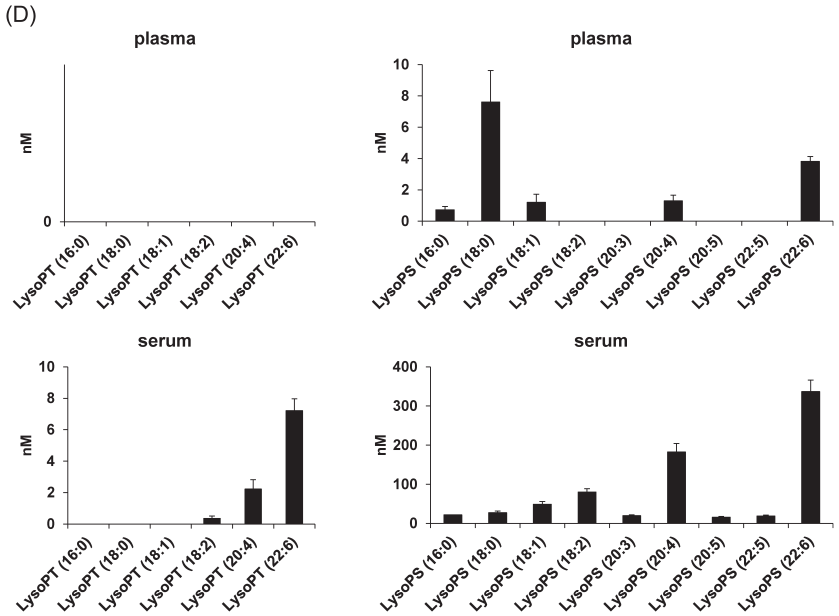

Fig. 3. Distribution of LysoPT and LysoPS in various mouse tissues.

(A) Concentrations of LysoPT (upper) and LysoPS (lower) species in tissues. (B and C) Concentrations of LysoPT (B) and LysoPS (C) species in A were shown for each tissue. (D) Concentrations of LysoPT and LysoPS species in plasma and serum. The values are the means+SD obtained from 3 mice. The values of the concentrations of each LysoPT and LysoPS species are shown in Table 3 (n=3, values are means+SD).

Table 3. Tissue concentrations of LysoPT and LysoPS species

Tissue	LysoPT (16:0)	LysoPT (18:0)	LysoPT (18:1)	LysoPT (18:2)	LysoPT (20:4)	LysoPT (22:6)
brain	N.D.	N.Q.	N.D.	N.D.	N.Q.	0.014 ± 0.008
thymus	N.D.	0.006 ± 0.002	N.Q.	N.Q.	N.Q.	N.Q.
heart	N.D.	0.014 ± 0.010	N.D.	N.D.	N.Q.	0.017 ± 0.008
lung	N.Q.	0.009 ± 0.006	N.Q.	N.Q.	N.Q.	N.Q.
liver	N.Q.	0.009 ± 0.002	N.D.	N.Q.	0.011 ± 0.003	0.011 ± 0.003
spleen	N.Q.	0.016 ± 0.008	N.Q.	N.Q.	N.Q.	0.005 ± 0.001
kidney	0.015 ± 0.004	0.064 ± 0.036	N.Q.	N.Q.	0.041 ± 0.008	0.006 ± 0.003
stomach	0.099 ± 0.043	0.406 ± 0.196	0.074 ± 0.030	N.Q.	0.005 ± 0.002	N.Q.
small-intestine	N.Q.	0.042 ± 0.013	N.D.	0.018 ± 0.002	0.021 ± 0.001	0.011 ± 0.001
large-intestine	0.005 ± 0.003	0.114 ± 0.097	0.012 ± 0.005	0.017 ± 0.001	0.019 ± 0.005	0.015 ± 0.006
mascle	N.Q.	0.009 ± 0.005	N.D.	N.D.	N.Q.	0.009 ± 0.001
skin	N.Q.	0.021 ± 0.003	N.Q.	N.Q.	N.Q.	N.Q.

Tissue	LysoPS (16:0)	LysoPS (18:0)	LysoPS (18:1)	LysoPS (18:2)	LysoPS (20:3)	LysoPS (20:4)	LysoPS (20:5)	LysoPS (22:5)	LysoPS (22:6)
brain	0.089 ± 0.012	1.133 ± 0.287	0.663 ± 0.156	0.009 ± 0.002	0.025 ± 0.011	0.130 ± 0.026	N.Q.	0.021 ± 0.010	7.313 ± 3.571
thymus	0.108 ± 0.020	1.088 ± 0.193	0.177 ± 0.028	0.075 ± 0.005	0.068 ± 0.008	0.117 ± 0.004	N.Q.	0.064 ± 0.005	0.297 ± 0.012
heart	0.010 ± 0.004	0.377 ± 0.099	0.031 ± 0.002	0.024 ± 0.006	0.008 ± 0.002	0.033 ± 0.010	N.Q.	0.018 ± 0.004	0.683 ± 0.210
lung	0.165 ± 0.031	1.029 ± 0.264	0.236 ± 0.035	0.087 ± 0.007	0.066 ± 0.001	0.198 ± 0.015	0.010 ± 0.003	0.091 ± 0.012	0.339 ± 0.027
liver	0.772 ± 0.123	2.548 ± 0.402	0.108 ± 0.012	0.098 ± 0.001	0.048 ± 0.008	1.032 ± 0.232	0.098 ± 0.022	0.054 ± 0.006	3.316 ± 0.536
spleen	0.196 ± 0.053	1.545 ± 0.344	0.230 ± 0.037	0.212 ± 0.026	0.061 ± 0.008	0.342 ± 0.012	0.026 ± 0.002	0.102 ± 0.016	0.634 ± 0.058
kidney	1.532 ± 0.182	5.740 ± 2.019	0.371 ± 0.036	0.443 ± 0.073	0.113 ± 0.018	2.485 ± 0.442	0.215 ± 0.036	0.079 ± 0.011	1.032 ± 0.212
stomach	9.288 ± 3.309	106.688 ± 37.900	8.402 ± 3.137	0.544 ± 0.128	0.046 ± 0.004	0.281 ± 0.015	0.016 ± 0.008	0.442 ± 0.188	0.485 ± 0.053
small-intestine	0.214 ± 0.038	4.706 ± 0.727	0.359 ± 0.046	1.191 ± 0.114	0.152 ± 0.016	0.361 ± 0.028	0.031 ± 0.011	0.077 ± 0.008	0.577 ± 0.043
large-intestine	0.259 ± 0.190	10.557 ± 9.512	0.751 ± 0.280	0.815 ± 0.089	0.240 ± 0.071	0.354 ± 0.095	0.020 ± 0.001	0.098 ± 0.060	0.830 ± 0.276
mascle	0.067 ± 0.005	0.614 ± 0.178	0.097 ± 0.021	0.023 ± 0.000	0.006 ± 0.001	0.019 ± 0.002	N.Q.	0.020 ± 0.002	0.373 ± 0.052
skin	0.150 ± 0.047	2.161 ± 0.454	0.457 ± 0.103	0.193 ± 0.045	0.042 ± 0.016	0.139 ± 0.026	N.Q.	0.064 ± 0.007	0.348 ± 0.071

Data are mean±SD (n=3). NQ not quantified ND not detected.

whereas in serum, C20:4- and C22:6-LysoPS were the main LysoPS species. This suggests that the synthetic pathways of LysoPS (and possibly those of LysoPT) differ between serum and plasma.

Discussion

There has been no evidence for the *in vivo* presence of LysoPT, since it was pharmacologically identified as a synthetic LysoPS analogue[5,6]. Our present results demonstrate that LysoPT is present in several mouse tissues and the blood. We changed the MS instrument and optimized the method for LysoPT analysis, which was also successfully applied to the detection of LysoPS. In TSQ Quantiva system (Thermo Fischer scientific), the lens instructed in the ion source in front of Q1 improved the removal efficiency of neutral molecules. As a result, the background was lowered, and the signal-to-noise ratio was improved, enabling the detection of LysoPT in biological samples. The LLOQ was 100 pm for both LysoPT and LysoPS (except for C18:1-LysoPT LLOQ, which is 500 pm), which is 5−20 times more sensitive than the method of Koistinen KM et al.[14] and 20−100 times sensitive than our previous method[13]. The previous methods were not sensitive enough to detect LysoPS or LysoPT in biological fluids such as plasma and serum. The total LysoPS concentrations in plasma and serum were 10−20 nM and 700−800 nM, respectively. The recent identification of four GPCRs specific to LysoPS[15−17] has indicated that LysoPS is an emerging lysophospholipid mediator with multiple biological roles like LPA and sphingosine 1-phosphate (S1P). Interestingly, LPA also showed similar nM plasma concentration to those of LysoPS[18], and the concentration is much lower than the effective concentration (EC_{50}) values for LysoPS receptors[16,17], providing further evidence that LysoPS behaves as a local lysophospholipid mediator. Higher levels of LysoPT and LysoPS were detected in serum than in plasma, indicating that they are lipid mediators produced upon platelet activation, as was indicated for LPA[19]. The present study also revealed that LysoPS and LysoPT have similar tissue distribution patterns, although LysoPT levels were much lower than LysoPS levels. Indeed, the amount of LysoPT is about 1/400th to 1/30th of LysoPS, depending on the tissues. It should be emphasized here that LysoPT induces a similar degree of degranulation from rat peritoneal mast cells at concentrations of several tenths of those of LysoPS[5]. Thus, LysoPT appears to exert its function *in vivo* despite its much lower concentration. Recently, four GPCRs were identified for LysoPS, i.e., LPS_1/GPR34, LPS_2/P2Y10, LPS_{2L}/A630033H20Rik, and LPS_3/GPR174[15,16]. However, LysoPT species (C16:0, C18:0 and C18:1) did not activate any of these receptors[6,16]. Thus, LysoPT is not a ligand for GPCR-type LysoPS receptors and has a role in activating mast cell degranulation.

The present study also revealed that the molecular species of LysoPT are similar to those of LysoPS. The only structural difference between LysoPT and LysoPS is that LysoPT has an additional methyl group attached to the serine residue of LysoPS. In addition, the tissue distribution patterns of LysoPT and LysoPS were quite similar (Fig. 3). Thus, we speculate that they share similar synthetic pathways. Interestingly, LysoPT species detected were found to have a fatty acid at the *sn*-1 position as judged by the detection system for *sn*-1/*sn*-2 lysophospholipids[13]. PT, the most likely precursor of LysoPT, is widely distributed in various species[10−12]. These notions indicate that LysoPT is produced from PT by phospholipase A_2 like LysoPS from PS. In a biological membrane, PS is mainly located in the inner leaflet of the plasma membrane. Thus, PT may show a similar bilayer distribution pattern in biological membranes. Further studies are required to understand the biological significance of LysoPTs. However, the analytical method described herein clearly shows that LysoPT is present both *in vivo* and *in vitro*.

Acknowledgments

This work was supported by AMED-LEAP (21gm0010004h9905) and KAKENHI (20K21379), both for JA.

Conflict of Interest

None to be declared.

References

1) Martin TW, Lagunoff D: Interactions of lysophospholipids and mast cells. *Nature* 279: 250−252, 1979.
2) Smith GA, Hesketh TR, Plumb RW, Metcalfe JC: The exogenous lipid requirement for histamine release from rat peritoneal mast cells stimulated by concanavalin A. *FEBS Lett* 105: 58−62, 1979.
3) Horigome K, Tamori-Natori Y, Inoue K, Nojima S: Effect of serine phospholipid structure on the enhancement of concanavalin A-induced degranulation in rat mast cells. *J*

Biochem 100: 571−579, 1986.

4) Bruni A, Bigon E, Battistella A, Boarato E, Mietto, L, Tiffany G: Lysophosphatidylserine as histamine releaser in mice and rats. *Agents Actions* 14: 619−625, 1984.
5) Iwashita M, Makide K, Nonomura T, Misumi Y, Otani Y, et al: Synthesis and evaluation of lysophosphatidylserine analogues as inducers of mast cell degranulation. Potent activities of lysophosphatidylthreonine and its 2-deoxy derivative. *J Med Chem* 52: 5837−5863, 2009.
6) Kishi T, Kawana H, Sayama M, Makide K, Inoue A, et al: Identification of lysophosphatidylthreonine with an aromatic fatty acid surrogate as a potent inducer of mast cell degranulation. *Biochem Biophys Rep* 8: 346−351, 2016.
7) Yokoyama K, Kubo I, Inoue K: Phospholipid degradation in rat calcium ionophore-activated platelets is catalyzed mainly by two discrete secretory phospholipase As. *J Biochem* 117: 1280−1287, 1995.
8) Aoki J, Inoue A, Make K, Saiki N, Arai H: Structure and function of extracellular phospholipase A_1 belonging to the pancreatic lipase gene family. *Biochimie* 89: 197−204, 2007.
9) Murakami M, Taketomi Y, Sato H, Yamamoto K: Secreted phospholipase A2 revisited. *J Biochem* 150: 233−255, 2011.
10) Omori T, Honda A, Mihara H, Kurihara T, Esaki N: Identification of novel mammalian phospholipids containing threonine, aspartate, and glutamate as the base moiety. *J Chromatogy B Analyt Technol Biomed Life Sci* 879: 3296−3302, 2011.
11) Mitoma J, Kasama T, Furuya S, Hirabayashi Y: Occurrence of an unusual phospholipid, phosphatidyl-L-threonine, in cultured hippocampal neurons. Exogenous L-serine is required for the synthesis of neuronal phosphatidyl-L-serine and sphingolipids. *J Biol Chem* 273: 19363−19366, 1998.
12) Arroyo-Olarte RD, Brouwers JF, Kuchipudi A, Helms JB, Biswas A, et al: Phosphatidylthreonine and lipid-Mediated control of parasite virulence. *PLos Biol* 13: e1002288, 2015.
13) Okudaira M, Inoue A, Shuto A, Nakanaga K, Kano K, et al: Separation and quantification of 2-acyl-1-lysophospholipids and 1-acyl-2-lysophospholipids in biological samples by LC-MS/MS. *J Lipid Res* 55: 2178−2192, 2014.
14) Koistinen KM, Suoniemi M, Simon H, Ekroos K: Quantitative lysophospholipidomics in human plasma and skin by LC-MS/MS. *Anal Bional Chem* 407: 5091−5099, 2015.
15) Sugo T, Tachimoto H, Chikatsu T, Murakami Y, et al: *Biochem Biophys Res Commun* 341: 1078−1087, 2006.
16) Inoue A, Ishiguro J, Kitamura H, Arima N, Okutani M, et al: TGFα shedding assay: An accurate and versatile method for detecting GPCR activation. *Nat Methods* 9: 1021−1029, 2012.
17) Kitamura H, Makide K, Shuto A, Okubo M, Inoue A, et al: GPR34 is a receptor for lysophosphatidylserine with a fatty acid at the *sn*-2 position. *J Biochem* 151: 511−518, 2012.
18) Kano K, Matsumoto H, Kono N, Kurano M, Yatomi Y, et al: Suppressing postcollection lysophosphatidic acid metabolism improves the precision of plasma LPA quantification. *J Lipid Res* 62: 100029, 2021.
19) Gerrard JM, Kindom SE, Peterson DA, Peller J, Krantz KE, et al: Lysophosphatidic acids. Influence on platelet aggregation and intracellular calcium flux. *Am J Pathol* 96: 423−438, 1979.